Single-Walled Carbon Nanotube Surface Control of Complement Recognition and Activation

Alina J. Andersen,[†] Joshua T. Robinson,[‡] Hongjie Dai,[‡] A. Christy Hunter,[§] Thomas L. Andresen,[⊥] and S. Moein Moghimi[†,∥,*]

[†]Centre for Pharmaceutical Nanotechnology and Nanotoxicology, Faculty of Health and Medical Sciences, University of Copenhagen, DK-2100 Copenhagen Ø, Denmark, [‡]Department of Chemistry, Stanford University, Keck Science Building, 380 Roth Way, Stanford, California 94305, United States, [§]School of Pharmacy and Pharmaceutical Sciences, University of Manchester, Stopford Building, Oxford Road, Manchester M13 9PT, United Kingdom, [⊥]Department of Micro- and Nanotechnology, Technical University of Denmark, 2800 Kgs. Lyngby, Denmark, and [∥]NanoScience Centre, University of Copenhagen, DK-2100 Copenhagen Ø, Denmark

ABSTRACT Carbon nanotubes (CNTs) are receiving considerable attention in site-specific drug and nucleic acid delivery, photodynamic therapy, and photoacoustic molecular imaging. Despite these advances, nanotubes may activate the complement system (an integral part of innate immunity), which can induce clinically significant anaphylaxis. We demonstrate that single-walled CNTs coated with human serum albumin activate the complement system through C1q-mediated classical and the alternative pathways. Surface coating with methoxypoly(ethylene glycol)-based amphiphiles, which confers solubility and prolongs circulation profiles of CNTs, activates the complement system differently, depending on the amphiphile structure. CNTs with linear poly(ethylene glycol) amphiphiles trigger the lectin pathway of the complement through both L-ficolin and mannan-binding lectin recognition. The lectin pathway activation, however, did not trigger the amplification loop of the alternative pathway. An amphiphile with branched poly(ethylene glycol) architecture also activated the lectin pathway but only through L-ficolin recognition. Importantly, this mode of activation neither generated anaphylatoxins nor induced triggering of the effector arm of the complement system. These observations provide a major step toward nanomaterial surface modification with polymers that have the properties to significantly improve innate immunocompatibility by limiting the formation of complement C3 and C5 convertases.

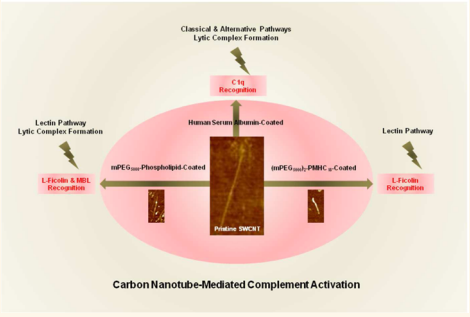

KEYWORDS: carbon nanotubes · complement system · L-ficolin · methoxy(polyethylene glycol)-phospholipid · poly(maleic anhydride-*alt*-1-octadecene)

Carbon nanotubes are graphene sheets rolled up into hollow cylinders with different aspect ratios and anisotropic characteristics.[1,2] These are divided into two groups, which includes single-walled carbon nanotubes (SWCNTs) and multiwalled species, consisting of a minimum of two concentric SWCNTs with an interlayer separation of around 0.34 nm. Carbon nanotubes exhibit unique electronic, photonic, mechanical, and chemical properties, which makes them attractive exploratory candidates for biological investigation.[3] Indeed, during the past few years, carbon nanotubes, although not biodegradable and which are not readily eliminated from the body, have received increasing attention in site-specific drug and nucleic acid delivery, photodynamic therapy, *in vivo* fluorescence imaging in the second near-infrared (NIR-II) window, and photoacoustic molecular imaging.[3−16] In particular, the deep penetration and low scattering of NIR-II photons emitted by SWCNT fluorescence open up a new exciting opportunity toward a high-resolution real-time *in vivo* imaging modality.[14−16]

Pristine carbon nanotubes are insoluble in nearly all aqueous solvents and biological fluids. Accordingly, there have been many measures in terms of surface treatment and functionalization strategies to render nanotubes readily dispersible.[4,5,9,17−24] Covalent functionalization,[17−20] however, may not sufficiently preserve the intrinsic physical properties of SWCNTs, such as near-infrared fluorescence and Raman scattering necessary for biomedical imaging and dynamic tracing. Accordingly, surface adsorption of polymeric amphiphiles such as methoxypoly(ethylene glycol)-phospholipid (mPEG-PL) has

* Address correspondence to moien.moghimi@sund.ku.dk.

Received for review September 4, 2012 and accepted January 9, 2013.

Published online January 09, 2013
10.1021/nn3055175

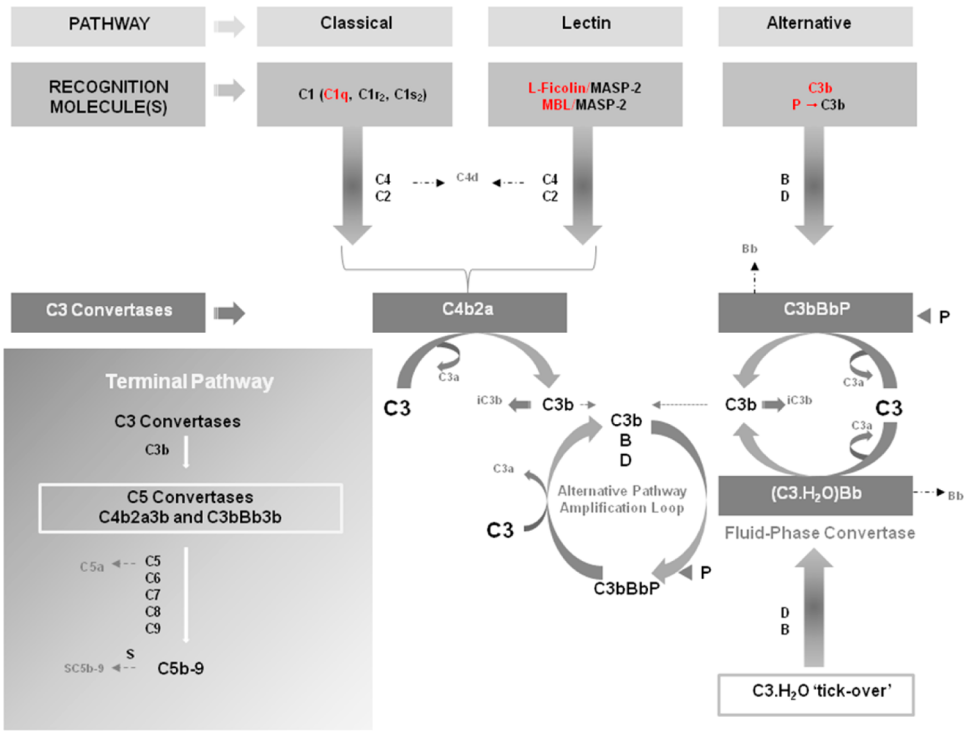

Figure 1. Complement recognition molecules and complement activation pathways. Key complement recognition molecules are shown in red. The cartoon shows sequential activation of complement components for each pathway as well as measurable pathway-dependent complement activation products (*e.g.*, C4d, Bb, iC3b, C3a, C5a, SC5b-9). Properdin (P) has dual roles. It acts not only as a pattern recognition molecule capable of activating the alternative pathway but also as a stabilizer of the alternative pathway convertase C3bBb, preventing its rapid dissociation by complement regulatory proteins. The inset represents the terminal pathway of the complement system and sequential activation of the complement proteins leading to the assembly of the lytic complex C5b-9 (also known as the membrane attack complex). In the fluid phase, S-protein (vitronectin) binds to C5b-9 and prevents interaction with membranes. Natural complement inhibitors and complement regulatory proteins are not shown in the scheme. MBL = mannan-binding lectin; MASP-2 = mannose-binding protein-associated serine protease-2.

become a useful strategy not only for forming highly stable SWCNT dispersions but also for imparting subsequent functionality and prolonging nanotube blood circulation profiles.[4,5,9,10,23,24] Indeed, PEGylation is an established approach that confers resistance to rapid nanoparticle clearance by blood monocytes and macrophages in direct contact with the blood.[25,26] This offers an unprecedented opportunity for targeting nanotubes to other vascular elements and targets beyond, depending on anatomical, ultrastructural, and pathophysiological processes.[25−27]

A number of molecular and functional studies have shown that nanoparticle PEGylation and surface modification with other related nonionic polymeric amphiphiles may not necessarily confer compatibility with the innate immune system.[26−37] This is due partly to gradual loss of the amphiphile from the surface and partly to the differential binding of complement recognition molecules depending on the bound polymer/amphiphile architecture. The complement system is an integral part of innate immunity and acts as a first line of defense against intruders, which can be activated through three general pathways (classical, lectin, and alternative pathways) following surface binding of a number of complement recognition molecules (Figure 1).[38,39] Although complement activation can prime the surface of intruders (including man-made nanoparticles) with opsonic complement fragments (C3b, iC3b) for recognition and clearance by phagocytic cells, its inadvertent activation may induce acute "allergic-like" reactions and anaphylaxis.[32,39] Two studies have shown that both pristine and PEGylated carbon nanotubes can trigger complement activation in human serum.[35,40] Pristine nanotubes initiated complement activation through the classical pathway,[40] but these observations may be due to the presence of large amounts of nanotube bundles and aggregates that could interact with the cationic globular head of the C1q molecule. In a separate study, PEGylated (PEG_{5000}) nanotubes were shown to trigger a complement system through the lectin pathway, but the underlying mechanistic aspects still remain to be revealed.[35] The latter observation, however, is interesting since surface concentration of the immobilized PEG_{5000} is well below the threshold of soluble surfactant quantities necessary for triggering complement activation.[35,41] This strongly suggests an important role for the surface PEG architecture in attracting different complement recognition molecules. Accordingly, we have examined the role of key complement recognition molecules in initiation and

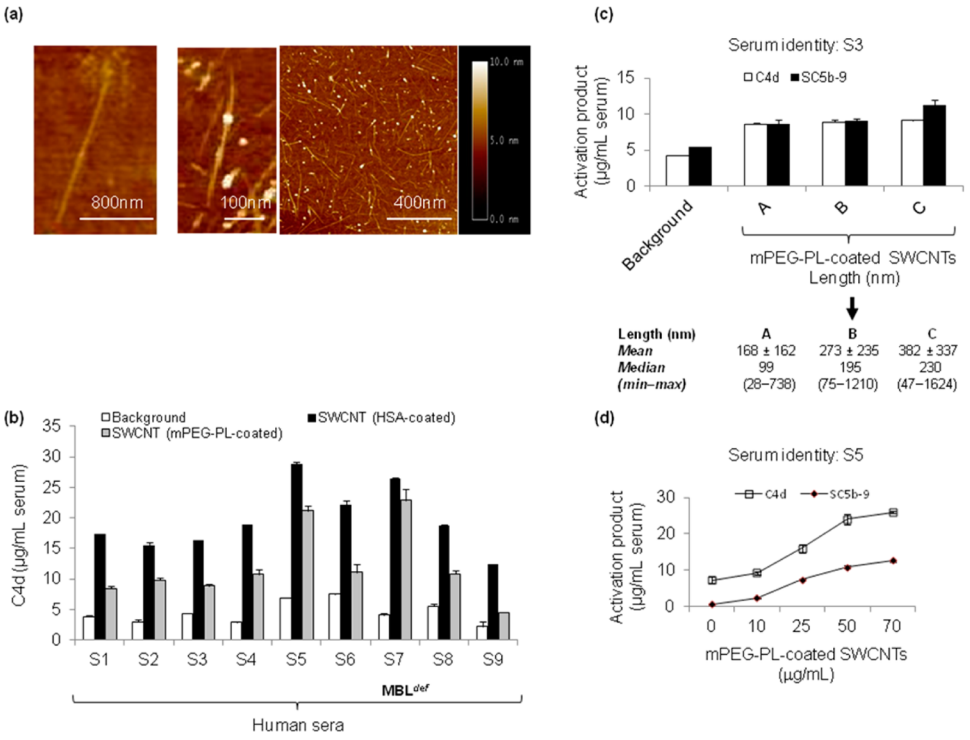

Figure 2. SWCNT-mediated activation of calcium-sensitive pathways and the terminal arm of the complement system. (a) Atomic force microscope images of SWCNTs. The left panel represents an image of a pristine SWCNT showing a uniform height along the structure. The right panel is representative images of $mPEG_{5000}$-PL-coated nanotubes. The middle panel shows a magnified view of a typical mPEG-PL-coated SWCNT; the non-uniform height along the surface is attributed to the presence of the mPEG-PL coating. (b) Nanotube-mediated cleavage of the C4-protein in sera of nine different individuals. Serum 7 (S7) is genetically deficient in mannan-binding lectin (MBL). The mPEG-PL-coated nanotubes were 273 ± 235 nm long (type B); HSA-coated nanotubes were of equivalent length. The final concentration of both nanotube types in the incubation was 70 μg carbon/mL. With the exception of S7, $p < 0.05$ in all cases of head-to-head comparison between the HSA- and mPEG-PL-coated nanotubes. Also, $p < 0.05$ when comparing each nanotube incubation to its respective background. (c) Effect of $mPEG_{5000}$-PL-coated SWCNT length on complement activation. Nanotube concentration was 70 μg carbon/mL. SC5b-9 is an established marker of the terminal pathway of complement (the effector arm) and representative of the activation of the whole complement cascade. (d) Effect of nanotube (type B) concentration on elevation of complement activation products. As positive control, zymosan (1 mg/mL) activated a complement more than 10-fold above background in all nine tested sera (SC5b-9 measurement) (data not shown).

triggering of different complement pathways by human serum albumin (HSA)-coated as well as linear and branched mPEG-amphiphile-coated pristine SWCNTs.

RESULTS AND DISCUSSION

Pristine SWCNTs (Figure 2a, left panel) are strongly aggregated, highly hydrophobic, and do not disperse in aqueous buffers. In accordance with earlier studies,[5,23] $mPEG_{5000}$-PL treatment conferred nanotube stabilization and formed highly stable aqueous dispersions. Surface deposition of $mPEG_{5000}$-PL on nanotubes was confirmed by an atomic force microscope (Figure 2a, right panel). Since HSA is the most abundant serum protein that binds hydrophobic surfaces readily,[26,42,43] it was also used to generate stable nanotube dispersions.

We initially investigated the effect of nanotube characteristics on triggering calcium-sensitive complement pathways (classical and lectin pathways) and the effector arm (terminal pathway) of the complement system. These were performed by measuring nanotube-mediated serum rises of C4d (a fluid-phase split product of C4, which is released by complement control protein C4bp and factor I, and an established marker of both classical and lectin pathways) and SC5b-9 (a nonlytic soluble marker of the terminal pathway of the complement and a sensitive measure of the activation of the whole complement cascade) levels, respectively.[31,36] The results in Figure 2b demonstrate that both HSA-coated and mPEG-PL-coated SWCNT species of equivalent length were able to raise C4d levels significantly above their respective background in all nine tested human sera, including a serum (S7) genetically deficient in mannan-binding lectin (MBL), which is one of the key primary complement recognition proteins that triggers lectin pathway activation.[38,44] All sera were devoid of IgG and IgM antibodies reactive toward the amphiphiles as tested by agglutination assay using the respected PEGylated autologous red blood cells.[41,45] Since antibodies can trigger complement activation through subsequent C1q binding,[38] this eliminates the role of anti-PEG antibodies in complement activation.[45] With the exception of the MBL-deficient (MBL^{def}) serum, mPEG-PL-coated nanotubes were significantly less efficient ($p < 0.05$) in triggering C4 cleavage (and hence C4d

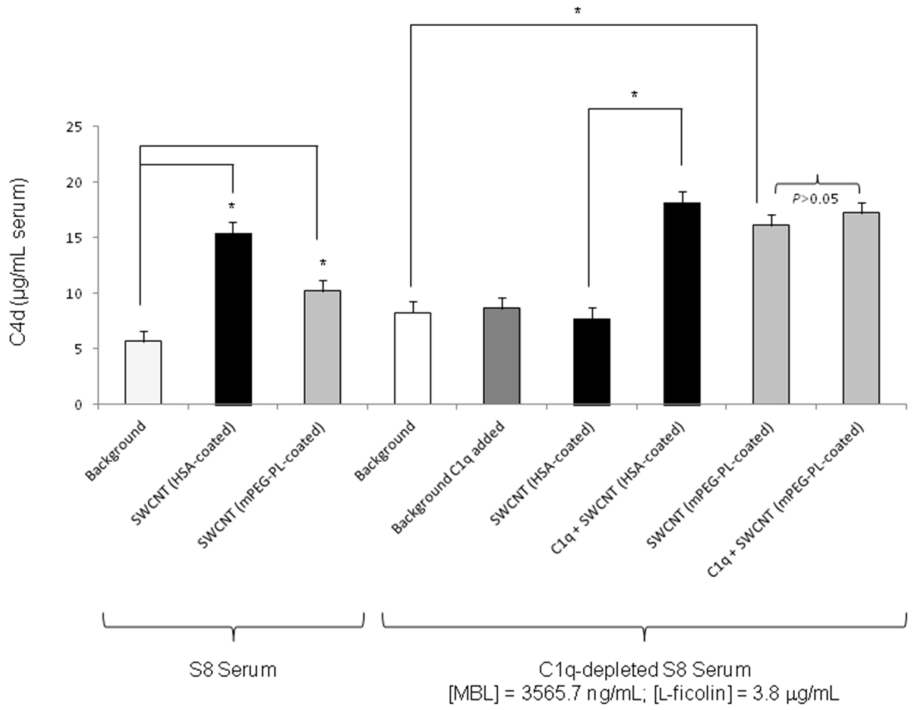

Figure 3. Differential effect of nanotube coating on C1q recognition and activation of the classical pathway. The mPEG$_{5000}$-PL-coated nanotubes were of type B, and HSA-coated nanotubes were of the same length as type B species. The final concentration of nanotubes in the incubation was 70 μg carbon/mL; *p < 0.05.

generation) in all tested sera compared with HSA-coated nanotubes. This lower detectable level of the fluid-phase C4d in sera treated with mPEG-PL-coated SWCNTs was not due to nonspecific binding of generated C4d to the nanotube surface (data not shown; see Materials and Experiments).

We next examined the effect of nanotube length on complement activation and restricted these studies to the mPEG-PL-coated species. The results in Figure 2c indicate that all nanotubes generate similar quantities of the complement activation products C4d and SC5b-9 irrespective of their length (average lengths of 168 $\pm$ 162, 273 $\pm$ 235, and 382 $\pm$ 337 nm, respectively). Since our earlier complement activation studies were with the mPEG-PL-coated nanotubes of mid-range length (type B, 273 $\pm$ 235 nm),[35] subsequent mechanistic studies were limited to this population. The results in Figure 2d show the effect of type B mPEG-PL-coated nanotube concentration on complement activation where the increasing concentration of nanotubes increased the level of complement activation products.

Role of the Classical Pathway. The first component of the classical pathway of complement is C1, a pattern recognition complex, which is composed of a single C1q molecule with a cationic globular head, bound to two molecules, the zymogens C1r and C1s.[38,46] The classical pathway is initiated by binding of the C1q head either to antigen–antibody complexes or to other pattern recognition molecules (*e.g.*, C-reactive protein) or directly to the surfaces of pathogens, nanoparticles, senescent, or damaged cells.[46] Following binding, C1q may undergo a conformational change, which results in a Ca^{2+}-dependent activation of C1r, which in turn cleaves its associated C1s to generate an active serine protease that acts on two natural substrates, C4 and C2. This in turn results in the formation of the classical pathway C3 convertase (C4b2a) (Figure 1).[46]

Two earlier studies have demonstrated C1q binding to pristine carbon nanotubes of different morphology,[40,47] but in one study, C1q binding was suggested to trigger complement activation.[40] Accordingly, we compared the role of C1q in activation of the classical pathway by both HSA- and mPEG-PL-coated SWCNTs. For this purpose, we depleted C1q from a typical responsive serum to nanotubes (serum S8) and refer to this as C1q^{dpl} serum. This treatment resulted in total abolition of HSA-coated CNT-mediated complement activation since serum levels of both C4d (Figure 3) and SC5b-9 (not shown) were comparable with the background levels. Complement activation by HSA-coated SWCNTs, however, was restored following addition of physiological levels of C1q (180 μg/mL). The C1q-depleted serum preparation also contained physiological levels of lectin pathway initiators and exhibited full lectin pathway functionality. This eliminates a possible role for the lectin pathway-mediated cleavage of C4. Therefore, HSA-coated nanotubes activate complement through C1q recognition. Whether C1q binds to the surface-adsorbed HSA or to the exposed pristine domains is not clear, but comparative studies with near monodisperse polystyrene nanoparticles of 250 nm in size (polydispersity index = 1.05) demonstrated that

both uncoated and HSA-coated nanospheres (with coating at the top plateau of the HSA adsorption isotherm) activated complement through the C1q-mediated classical pathway (data not shown). Indeed, complement activation by HSA-coated nanospheres was in accord with our earlier observations.[43]

In contrast to HSA-coated nanotubes, the mPEG-PL-coated counterparts elevated C4d levels above the background in the $C1q^{dpl}$ serum, and addition of C1q had no effect on further C4d elevation (Figure 3). Similar results were obtained by prior incubation of mPEG-PL-coated nanotubes in 0.05% w/v HSA (not shown). We conclude that mPEG-PL-coated nanotubes, unlike their HSA-coated counterparts, predominantly raise serum C4d levels through activation of the lectin pathway. However, we cannot fully disregard C1q deposition on mPEG-PL-coated nanotubes, but based on these observations, possible surface-bound C1q molecules are unlikely to activate their associated C1r and C1s zymogens.

mPEG-PL-Coated Nanotube-Mediated Triggering of the Lectin Pathway. Activation of the lectin pathway typically proceeds following either the binding of serum MBL to mannose-expressing surfaces or the binding of serum L-ficolin (also known as ficolin-2, hucolin, elastin-binding protein, and P35) to surfaces rich with N-acetylated sugars or other acetylated compounds (Figure 1).[38,44] However, these functionalities for recognition by both MBL and ficolins are missing on the surface of mPEG-PL-coated nanotubes. Therefore, this raises an interesting question as how these nanotubes can trigger the lectin pathway. The binding of MBL or L-ficolin to an activating surface results in the conversion of their associated serine proteases zymogens [mannose-binding protein-associated serine proteases (MASP) 1, 2, and 3] to active proteolytic enzymes.[44] Activated MASP-2, however, is known to cleave C4, which in turn results in C2 cleavage and formation of a C3 convertase identical to that of the classical pathway.[44] It is also probable that nanotubes may activate MASP-2 directly and independent of MBL and/or ficolin binding and conformational changes.

We first assessed whether L-ficolin plays a role in mPEG-PL-coated SWCNT-mediated triggering of the lectin pathway. To do this, we eliminated the contribution of MBL in the lectin pathway activation by using a serum genetically deficient in MBL (MBL^{def} serum S7). This serum was also immunochemically depleted from C1q to further eliminate the role of C1q in complement activation in subsequent studies involving antibody addition. We further confirmed that the MBL^{def} C1q-depleted ($MBL^{def}/C1q^{dpl}$) serum contained physiological concentrations of L-ficolin (4.2 μg/mL). The results in Figure 4a show that mPEG-PL-coated SWCNT-mediated C4d generation proceeds well in $MBL^{def}/C1q^{dpl}$ serum. Nanotube-mediated C4d generation, however, was abolished by addition of *N*-acetylglucosamine in a

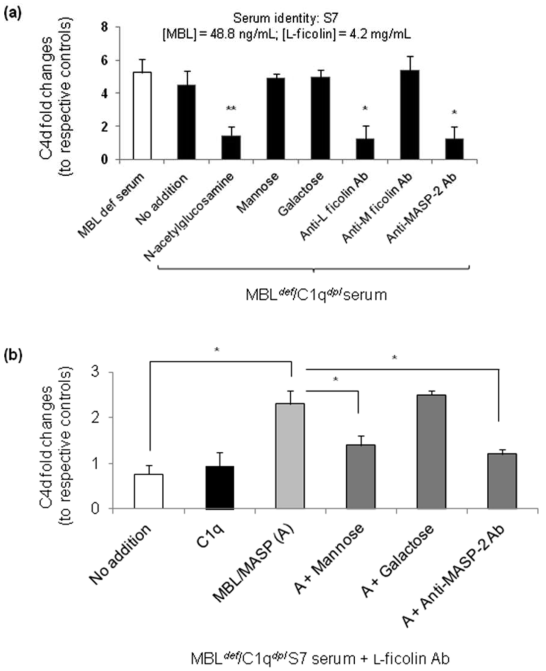

Figure 4. Activation of the lectin pathway of the complement system by $mPEG_{5000}$-PL-coated SWCNTs is both L-ficolin/MASP-2- and MBL/MASP-2-dependent. (a) Role of L-ficolin and MASP-2 in $mPEG_{5000}$-PL-coated nanotube-mediated triggering of the lectin pathway is confirmed in the S7 serum, which is genetically deficient in MBL (MBL^{def}) and following immunochemical depletion of C1q in this serum ($MBL^{def}C1q^{dpl}$). This serum contained physiological levels of L-ficolin (4.2 μg/mL). (b) Role of MBL and MASP-2 in nanotube-mediated complement activation is confirmed in $MBL^{def}C1q^{dpl}$ serum in the presence of L-ficolin antibodies. Type B $mPEG_{5000}$-PL-coated nanotubes were used throughout and at a final concentration of 70 μg carbon/mL; *$p < 0.05$, **$p < 0.01$. Ab = antibody.

millimolar range but not by D-mannose (a substrate for MBL)[41,48] and D-galactose (a nonantagonist) in $MBL^{def}/C1q^{dpl}$ serum. This strongly indicates a role for L-ficolin in lectin pathway activation since L-ficolin is known to express specificity only for sugars with N-acetylated groups.[41,48,49] Furthermore, nanotube-mediated C4d elevation was also abolished in the presence of anti-L-ficolin antibodies as well as anti-MASP-2 antibodies. The sensitivity to these antibodies indicates that the L-ficolin not only recognizes the surface of mPEG-PL-coated nanotubes but the binding activates MASP-2, which in turn cleaves C4.

In contrast to anti-L-ficolin antibodies, anti-M-ficolin antibodies exerted no effect on nanotube-mediated complement activation. This observation is in accord with the fact that M-ficolin is not typically present in serum.[50,51] It should be emphasized that the recombinant M-ficolin shares some similar ligands for binding as L-ficolin.[50,51] Since M-ficolin is localized mainly in secretory granules in the cytoplasm of monocytes, neutrophils, and type-II alveolar epithelial cells in the lung,[51] these cells may play a critical role in mPEG-coated or glycosylated[34,52] (*e.g.*, glycolipid-coated or grafted) nanotube-mediated inflammatory reactions through local complement activation.

TABLE 1. Height Analysis of SWCNTs with Different mPEG-Amphiphile Coating

	$mPEG_{5000}$-PL		$mPEG_{5000}$-$PMHC_{18}$	
height (H)	mean (nm) ± SD	median (nm) (min−max)	mean (nm) ± SD	median (nm) (min−max)
H1 (edge 1)	2.43 ± 1.54	1.53 (1.08−4.88)	3.32 ± 1.67	2.72 (1.80−7.82)
H2 (center)	1.80 ± 0.52	1.84 (1.06−2.99)	2.87 ± 1.62	2.16 (1.29−6.22)
H3 (edge 2)	1.74 ± 0.51	1.86 (0.91−2.50)	3.77 ± 1.87	3.33 (1.25−8.32)
H1 + H2 + H3	1.99 ± 1.01		3.18 ± 1.73	

Having established a key role for L-ficolin recognition, we next assessed whether MBL can also recognize the surface of mPEG-PL-coated nanotubes and subsequently initiate lectin pathway activation. Accordingly, we assessed complement activation by mPEG-PL-coated nanotubes in $MBL^{def}/C1q^{dpl}$ serum in the presence of anti-L-ficolin antibodies, but following the addition of functional purified MBL/MASP-2 complexes. Indeed, the results in Figure 4b show a critical role for MBL/MASP-2 in C4 cleavage. This was further confirmed through suppression of C4d elevation following the addition of D-mannose (at millimolar range) and anti-MASP-2 antibodies, respectively. In addition to this, we were further able to eliminate a role for C1q in mPEG-PL-coated nanotube-mediated complement activation since addition of C1q to $MBL^{def}/C1q^{dpl}$ serum in the presence of anti-L-ficolin antibodies did not elevate C4d levels above the background (Figure 4b). Therefore, we conclude that both L-ficolin and MBL recognize the surface of mPEG-PL-coated nanotubes, resulting in activation of their associated MASP-2 zymogen. Atomic force microscope analysis (Table 1) attested to this by demonstrating that uneven coating is a practically inevitable effect of surface adsorption of mPEG-PL. Therefore, complement activation by mPEG-PL-coated nanotubes could indicate that the two lectin pathway initiators (MBL and L-ficolin) bind to areas with different levels of coating, PEG conformation, and mPEG-PL phases. For instance, some surface regions may promote deposition of mannosylated serum/plasma proteins (*e.g.*, apolipoproteins),[35,40] where following conformational changes the exposed mannose groups may serve as templates for MBL binding and hence activation of MASP-2. Indeed, apolipoprotein deposition from serum on carbon nanotube surfaces has been demonstrated previously.[40] On the other hand, surface-projected mPEG chains, depending on their local density and proximity, may transiently resemble structural motifs of D-mannose and other sugars/acetylated compounds that aid either MBL or L-ficolin deposition.[39] Interestingly, the extent of mPEG-PL surface modification in these experiments was sufficient to prevent complement activation through C1q activity. These observations are also similar to the complement activation processes of block copolymer poloxamine 908-coated polystyrene nanospheres, shown earlier by us,[36] where complement activation was switched from the C1q-mediated classical pathway to the lectin pathway when the surface density of the bound copolymer was increased to levels that resembled a "brush-like" configuration. Accordingly, further and more complex biophysical characterization studies are still necessary for assessing surface coating qualities with mPEG-PL in relation to their role in triggering the lectin pathway.

Finally, we also confirmed that HSA-coated nanotube-mediated activation of calcium-sensitive pathways of complement is purely C1q-dependent since no C4d elevation above background was detectable in $MBL^{def}/C1q^{dpl}$ serum restored with MBL/MASP-2 (data not shown).

C3 Conversion and the Role of the Alternative Pathway Turnover. Cleavage of C3 is the central step in the complement cascade where all complement activation pathways converge. The C4b2a convertase of both classical and lectin pathways cleaves the α chain of C3 to release anaphylatoxin C3a, from the amino-terminus; this exposes an internal thiolester bond in the α chain of C3b.[38] Approximately, 10% of C3 binds covalently to a complement-activating surface.[39] The thiolester of the majority of the activated C3 reacts with water, forming inactive fluid-phase C3b. Some C3b binds to C4b in C4b2a and acts as a platform for C5 binding.[38] The new complex, C4b2a3b, is the C5 convertase of classical and lectin pathways and is responsible for the release of the highly potent anaphylatoxin C5a from the amino-terminus of C5 and the major cleavage product C5b. The latter split product initiates the assembly of the cytolytic membrane attack complex by recruiting the terminal complement proteins (C6, C7, C8, and C9) (Figure 1).[38,39] Initiation of the alternative pathway activation requires the presence of preformed C3b or an autoactivated form of C3 (C3 "tick-over") known as $C3 \cdot H_2O$, along with complement factors B and D, resulting in the formation the fluid-phase alternative pathway convertase C3bBb (Figure 1). Whenever C3 is cleaved by ongoing complement activation through classical and lectin pathways (or even the alternative pathway), the generated C3b can bind factor B and subsequently increase alternative pathway turnover through more C3bBb convertase generation. This is known as the C3 feedback or amplification loop. Binding of properdin (or factor P) to C3bBb stabilizes the alternative pathway C3 convertases, extending their half-life from approximately 90 s to 15 min.

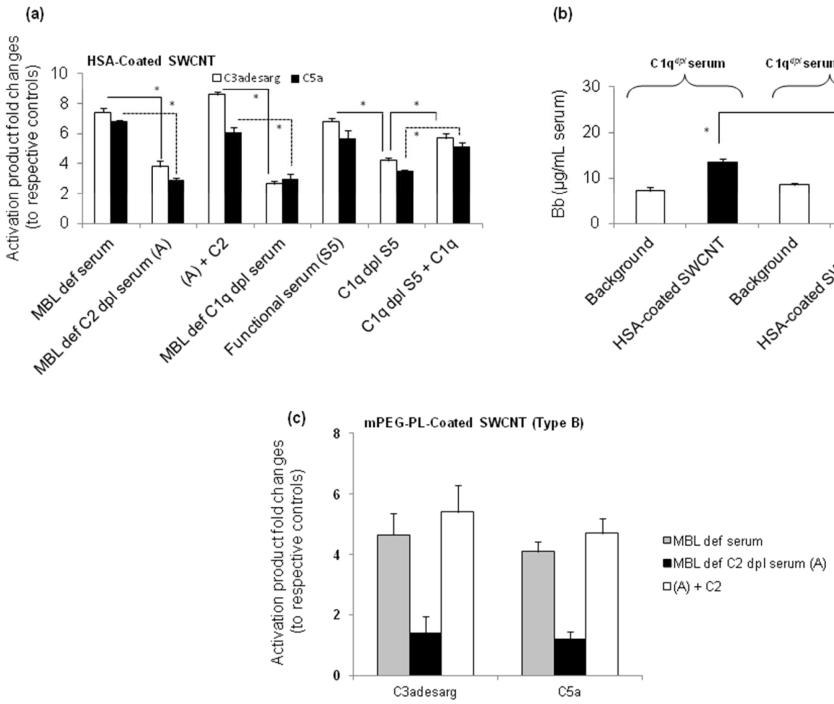

Figure 5. SWCNT-mediated anaphylatoxin C3a and C5a generation (a,c) and triggering of the amplification loop of the alternative pathway (b). In (a,c), C2 was immunochemically depleted from the MBL-deficient S7 serum. In (a,b), the normal S5 serum was used for immunochemical depletion of C1q. The final concentration of nanotubes was 70 μg carbon/mL; *$p < 0.05$.

In the presence of sufficient C3b, the alternative pathway C5 convertase C3bBb3b is also formed, resulting in C5 cleavage and subsequent assembly of the membrane attack complex.

HSA-coated nanotubes generated both C3a and C5a anaphylatoxins in $MBL^{def}/C2^{dpl}$, $MBL^{def}/C1q^{dpl}$, and $C1q^{dpl}$ sera (Figure 5a). These observations suggest that HSA-coated nanotubes can directly enhance alternative pathway turnover and independent of C1-mediated C4 cleavage and formation of the classical pathway C3 convertases. More anaphylatoxins, however, were generated when the physiological levels of C2 and C1q proteins were restored in $MBL^{def}/C2^{dpl}$ and $C1q^{dpl}$ sera, respectively. This may further suggest a role for the amplification loop of the alternative pathway in C3 conversion possibly through surface deposition/binding of C3b, C3bB, and C3bBb. Indeed, this is supported by serum rise of Bb levels in $C1q^{dpl}$ serum above the background following C1q restoration since Bb is an established marker of the alternative pathway activation (Figure 5b).

The results in Figure 5c show that mPEG-PL-coated nanotube-mediated lectin pathway activation in MBL^{def} serum can lead to generation of both C3a and C5a only in the presence of functional C2 since anaphylatoxin generation is abolished when C2 is immunochemically depleted but proceeds when C2 level is restored. This not only supports the notion that C3 cleavage is C4b2a-convertase-dependent but also indicates that a mPEG-PL-coated nanotube cannot trigger directly the alternative pathway and generate the alternative pathway convertase. In addition to this, mPEG-PL-coated nanotube-mediated activation of the lectin pathway, which generates C3b, also seems not to trigger the amplification loop of the alternative pathway[38] because no significant Bb levels were detectable above the background (data not shown). Accordingly, surface-bound C3b molecules either do not form C3bB complexes or such formed complexes remain insensitive to factor D-mediated cleavage of the bound factor B, and subsequent release of Bb by factor H, possibly arising from mPEG conformational constraint.

Another possibility that may increase alternative pathway turnover, but was not investigated, is direct binding of the pattern recognition molecule properdin to the nanotubes. Indeed, like the globular head of C1q, properdin is a highly cationic molecule.[53] Properdin is composed of identical 53 kDa protein subunits, where each subunit is rod-shaped and of 26 nm in length and 2.5 nm in diameter.[53] The properdin subunits may associate and form cyclic dimers, trimers, and tetramers that resemble rods, triangles, and squares, respectively.[53] These features make properdin a likely candidate for deposition on pristine nanotubes and subsequent enhancement of alternative pathway through C3b recruitment. As with M-ficolin, properdin is also stored in monocytes and neutrophils[54] and is released following stimulation with secondary mediators. Accordingly, properdin release may play a critical role in nanotube-mediated damage through direct binding as well as by stabilizing the alternative pathway convertases

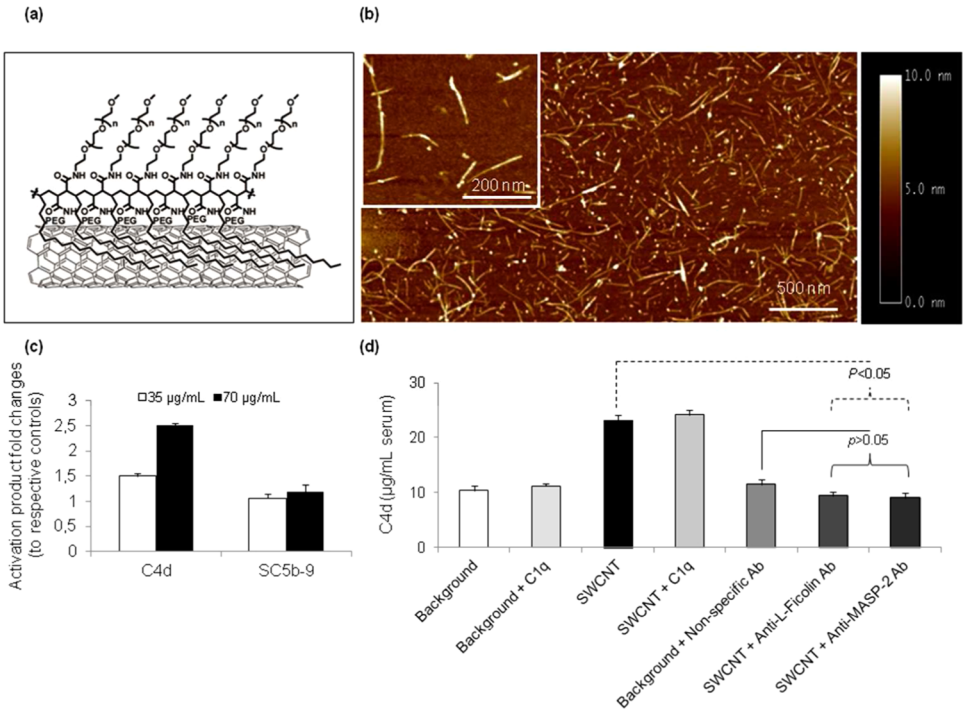

Figure 6. mPEG-PHMC$_{18}$-coated SWCNTs activate complement partially through the lectin pathway. (a) Idealized schematic representation of mPEG-PHMC$_{18}$-coated SWCNT. (b) Topographic atomic force microscope images of mPEG-PHMC$_{18}$-coated SWCNTs. The inset in (b) is a magnified view of the coated nanotubes. Note the extent of coating uniformity relative to that of mPEG-PL-coated nanotubes in Figure 1a. (c) Effect of nanotube concentration on C4d and SC5b-9 generation in serum, and (d) role of L-ficolin in activation of the lectin pathway by mPEG-PHMC$_{18}$-coated SWCNTs following immunochemical depletion of C1q from the serum (S8 serum as source). Nanotube characteristics: length 170 ± 76 nm; median 150 nm (min length = 60 nm, max length = 390 nm).

(an established property of this molecule). This will aid C5a generation and could inflict further damage.

SWCNT Coating with a Branched mPEG Amphiphile Does Not Trigger the Terminal Pathway of the Complement. We next sought to determine whether coating of nanotubes with a branched PEG copolymer with appropriate PEG distancing may induce better protein exclusion[55] and consequently diminish or abolish complement activation. Accordingly, we turned our attention to nanotube coating with poly(maleic anhydride-*alt*-1-octadecene) (PMHC$_{18}$), bearing two molecules of mPEG$_{5000}$ per unit of PMHC$_{18}$ (Figure 6a).[24] Atomic force microscopy studies confirmed nanotube coating by the branched mPEG-PMHC$_{18}$ copolymers (Figure 6b). This copolymer was shown earlier to have a strong tendency to adsorb onto the surface of SWCNTs by hydrophobic interactions, where coated nanotubes showed high stability to a range of pH values, salt conditions, and introduction of serum.[24] In contrast to mPEG-PL-coated nanotubes, the mPEG-PMHC$_{18}$-coated counterparts displayed increased height throughout the three measured regions (Table 1). The lowest height profile among mPEG-PMHC$_{18}$-coated nanotubes, however, far exceeds the highest measured height profile of mPEG-PL-coated SWCNTs. Higher structures of 6−8 nm were only present in mPEG-PMHC$_{18}$-coated species and more profound at the terminal regions (H1 and H3). This may be a reflection of considerably higher average molecular weight of the mPEG-PMHC$_{18}$ amphiphiles (1−2 MDa), with each molecule composed of more than 100 maleic anhydride units, compared with uniform-sized mPEG-PL conjugate molecules (~6 kDa). The presence of higher structures therefore indicates that only a fraction of the maleic anhydride units is in direct contact with the pristine surface, where this probability is highest at nanotube ends/edges. Since both types of amphiphiles are not covalently attached to SWCNTs, they could be moved slightly by the tip during imaging. Thus, the calculated heights may be underestimated.

As depicted in Figure 6c, mPEG-PMHC$_{18}$-coated nanotubes activated the complement system partially. The elevation of C4d levels again suggests a role for both classical and lectin pathways of complement, but C4 cleavage had no effect on the activation of the effector arm of the complement system since serum SC5b-9 levels remained comparable with the background. The lack of SC5b-9 generation closely matched low levels of C5a (not shown). Further studies in a C1q^{dpl} serum with physiological levels of both MBL and L-ficolin showed that C4 cleavage arises from lectin pathway activation and through L-ficolin recognition (Figure 6d). Indeed, C4d rises remained insensitive to C1q addition and were totally abolished in the presence of anti-L-ficolin and anti-MASP-2 antibodies. The latter observation eliminates MBL recognition-mediated

TABLE 2. Comparison of Complement Activation Pathways by Different Surface-Coated Carbon Nanotube Dispersions

nanotube type	recognition molecule	complement pathway[a]	lytic complex formation
HSA-coated	C1q	CP → AP (amplification loop)	yes
HSA-coated	C3b?	AP ("tick-over")	yes
$mPEG_{5000}$-PL-coated	L-ficolin and MBL	LP	yes
$(mPEG_{5000})_2$-$PMHC_{18}$-coated	L-ficolin	LP	no

[a] CP = classical pathway; AP = alternative pathway; LP = lectin pathway.

triggering of the lectin pathway. It is likely that the tertiary structure of the poly(maleic anhydride) backbone forces mPEG chains to remain ~10−15 Å apart,[24] an arrangement that has been previously shown to be the ideal spacing for better protein exclusion.[55] Such topological displays could either interfere with assembly of the C3 convertase C4b2a and/or C3b binding and explain these observations. The partial ability of complement triggering of $PMHC_{18}$-coated nanotubes is also consistent with their unprecedented long blood circulation profile compared with linear $mPEG_{5000}$-PL-coated SWCNTs[23,24] and presumably a reflection of limited opsonization by C3b and iC3b.[25,39] Accordingly, branched mPEG-$PMHC_{18}$-coated nanotubes are expected to exhibit better immune and hemodynamic safety features since generation of the C5a anaphylatoxin and multiprotein C5b-9 complexes remains negligible. Indeed, C5b-9 complexes have the capacity to elicit nonlytic stimulatory responses from vascular endothelial cells and modulate endothelial regulation of hemostasis and inflammatory cell recruitment.[56]

The preparation of mPEG-$PMHC_{18}$-coated nanotubes, however, generated shorter nanotubes (mean length = 170 ± 76 nm) compared with the type B mPEG-PL-coated nanotubes. Shorter nanotube lengths may affect conformational arrangements of the adsorbed $PMHC_{18}$ molecules more dramatically than the smaller mPEG-PL conjugates. Consequently, such arrangements may limit surface recognition by complement proteins and the extent of activation activation. Further experiments, however, are necessary to assess the effect of nanotube aspect ratios on projected mPEG-$PMHC_{18}$ architecture and complement activation.

CONCLUSIONS

We have shown that $mPEG_{5000}$-amphiphile coating of SWCNTs can modulate innate immunity through multiple paths (Table 2). First, it may reduce the absolute quantity of complement activation product generation compared with HSA-coated nanotubes. Second, it abolishes HSA-coated nanotube-mediated turnover of the alternative pathway. These observations are in line with the reported relatively prolonged circulation times of PEGylated SWCNTS since an alternative pathway can amplify C3 conversion in any type of complement activation and improve complement opsonization through C3b binding and hence phagocytic clearance.[39] Third, it activates the complement in different ways than HSA coating and specifically through L-ficolin and MBL recognition, but the lectin pathway activation does not trigger the alternative pathway amplification loop. Complement initiation by both L-ficolin and MBL is most likely a reflection of surface-assembled PEG architectural arrangements that transiently resemble structural motifs of the corresponding sugar substrates for these sensing molecules.[36,39] Indeed, our current surface analysis clearly demonstrated heterogeneity in mPEG-PL coating, but more advanced methodologies are required to assess the PEG conformation, coating density, and defects on different SWCNT populations. The resulting PEG coating density, however, is poorly controlled and heterogeneous in each SWCNT case, but in perhaps different ways, which subsequently triggers the complement system through different pathways. Nevertheless, inadvertent complement activation by PEGylated nanotubes remains a concern as it may still lead to acute "allergic-like" reactions through anaphylatoxin generation and C5b-9 modulation of hemostasis.[32,39] Indeed, both C3a and C5a over a generation might contribute to cutaneous reactions, respiratory and circulatory disturbances, and influence disease severity and eventually organ failure (*e.g.*, pulmonary dysfunction). However, through better surface PEGylation and PEG architectural arrangements, as in the case of branched mPEG-$PMHC_{18}$ conditioning, complement activation can be minimized and restricted to the initiation phase. Surprisingly, this mode of adsorption further eliminated MBL-mediated triggering of the lectin pathway. This is presumably a reflection of altered surface-projected mPEG chain arrangement in dissipating C3 convertase formation/activity. We conclude that this approach improves immune safety, which is also reflected in better circulation profiles of SWCNTs reported earlier.[24] Therefore, strategies that offer SWCNT surface modification with branched mPEG amphiphiles may prove an alternative solution for exploring the biological function and application of carbon nanotubes. This approach seems not to overactivate the innate arm of the immune system, which has a primary function of recognizing patterned structures. However, one drawback particularly with the branched mPEG-$PMHC_{18}$ is the high molecular weight of the poly(maleic anhydride) backbone, which limits the eventual copolymer excretion through kidneys, where the cutoff for glomerular filtration is 60 kDa.[25] These findings

are also applicable to better surface conditioning of hydrophobic nanoparticles, biomaterials, and implants with suitable branched mPEG-amphiphiles and improving their innate immunocompatibility.[57,58]

MATERIALS AND EXPERIMENTS

Materials. HiPCO SWCNTs were purchase from Carbon Nanotechnologies Inc. and used without further purification. DSPE-mPEG$_{5000}$ and mPEG$_{5000}$-NH$_2$ were obtained from Laysan Bio Inc. Procedures for synthesis, purification, and characterization of mPEG-poly(maleic anhydride-*alt*-1-octadecene) (mPEG-PMHC$_{18}$) were in accord with the previously established protocols.[24]

Stabilization of SWCNTs. Raw HiPCO SWCNTs (0.2 mg/mL) were sonicated in either 0.2 mM solution of DSPE-mPEG$_{5000}$ or 1 mg/mL of branched mPEG-PMHC$_{18}$ or 0.05% w/v of human serum albumin (HSA) for 1 h with a bath sonicator, followed by centrifugation at 22 000*g* for 6 h to remove aggregates.[23,24] Respective supernatants were collected and passed six times through a 100 kDa MWCO centrifuge filters and extensive washing with water (Millipore Amicon Ultra) as established earlier.[23,24]

Preparation of Stabilized SWCNTs with Fractionated Lengths. Surfactant (or protein)-stabilized SWCNTs underwent a density gradient fractionation in order to separate them by length. A similar procedure was previously established by Sun *et al.*[59] In this study, we used density gradients (0.5 mL) of 10, 20, 30, 40, and 60% iodixanol (Sigma Aldrich). Samples were centrifuged for 1 h at 300 000*g*, and fractions were collected from the top of the centrifuge tube.

Nanotube Characterization. UV−vis−NIR absorption spectrum of nanotube preparations was acquired by a Varian Cary 6000i spectrophotometer at λ = 808 nm.[23] A mass extinction coefficient of 46.5 L g^{-1} cm^{-1} was used to determine the nanotube concentration.[23] SWCNTs were further analyzed on silicon substrates by tapping-mode atomic force microscopy (Veeco Nanosage IIIa).[23,24] Silicon substrates were initially soaked with 0.6% APTES (3-aminopropyltriethoxysilane) to allow for higher concentration of nanotube deposition. SWCNTs (0.01 mg/mL) were soaked on the substrate for 15 min, then rinsed and imaged. The length distribution for each preparation was determined from 75 random SWCNT lengths. Pristine nanotubes were also imaged following treatment with 0.1% w/v sodium deoxycholate. The average height of the mPEG-coated nanotubes was determined by several random height profiles of the two edges and the center regions.

Preparation, Treatment, Characterization, and Storage of Human Sera. Blood was drawn from healthy Caucasian male and female volunteers (aged 25−40 years) according to approved local protocols. Blood was allowed to clot at room temperature, and serum was prepared, aliquoted, and stored at −80 °C. Serum samples were thawed and kept at 4 °C before incubation with test reagents. Serum concentration of mannan-binding lectin (MBL) was determined using the MBL-C4 complex ELISA kit (HyCult Biotechnology, The Netherlands), with a measurable concentration range of 0.41−100 ng/mL, following sample dilution.[41] The physiological concentrations of serum MBL are in the range of 3000−5000 ng/mL serum.[41] Individuals genetically deficient in MBL have serum MBL levels below 100 ng/mL. MBL/MASP-2 preparation and characterization were in accord with established procedures.[60] Human serum L-ficolin concentration was measured using the HK336 ELISA kit (HyCult Biotechnology, The Netherlands), with a measurable concentration range of 16−1000 ng/mL, following sample dilution. Sera were devoid of antibodies that may react with PEG as tested by agglutination assay using the respected PEGylated autologous red blood cells described in detail elsewhere.[41,45] For the assessment of the role of C1q and C4b2a convertases in complement activation, C1q and C2 were immunochemically depleted from some sera. This was achieved by incubating serum in 20 mM EDTA with mouse monoclonal anticomplement C1q or C2 antibodies, respectively, coupled to activated CNBr-sepharose. The complement hemolytic activity of C1q-depleted and C2-depleted sera was restored following the addition of C1q (180 μg/mL) and C2 (650 μg/mL), respectively, as well as divalent cations, as assessed by the hemolytic test using sheep erythrocytes sensitized with rabbit anti-sheep erythrocyte antibody.[41] The functional activity of classical, lectin, and the alternative pathways of complement was tested in all sera with Wielisa total complement screen kit (Lund, Sweden).[41]

Assays of *In Vitro* Complement Activation. To measure complement activation *in vitro*, we determined SWCNT-induced rise of serum complement activation product C4d, Bb, C3adesarg, C5a, and SC5b-9 using respective Quidel's (Quidel, San Diego) ELISA kits according to the manufacturer's protocols as described previously.[31,35,36,41] For measurement of complement activation, the reaction was started by adding the required quantity of SWCNTs to undiluted serum in Eppendorf tubes (either in duplicate or triplicate, depending on the experiment) in a shaking water bath at 37 °C for 30 min, unless stated otherwise. Reactions were terminated by addition of "sample diluent" provided with assay kit or saline containing 25 mM EDTA. SWCNT-induced rises of serum complement activation products were then measured following nanotube removal. Appropriate controls were also made by adding SWCNTs to saline for background correction in ELISA experiments. Control serum incubations contained saline (the same volume as nanotubes and other additions) for assessing background levels of complement activation products. To monitor the possible binding of complement activation products to the nanotube surfaces, we incubated SWCNTs with standard samples of the activation products.[35] The level of the standard activation products in the supernatant was then measured by the respective ELISA test and compared with control incubations in the absence of nanotubes. In some experiments, SWCNT-mediated complement activation was monitored following restoration of C1q, MBL/MASP-2, and C2 in the respected factor depleted or genetically deficient serum. SWCNT-induced complement activation was further monitored following pretreatment of selected sera with *N*-acetylglucosamine (25 mM), D-mannose (25 mM), D-galactose (25 mM), and monoclonal antibodies (mouse monoclonal antibodies against human L-ficolin, M-ficolin, and MASP-2 from HyCult Biotechnology, The Netherlands) or an irrelevant control antibody after appropriate dilutions. Zymosan (1 mg/mL) was used as a positive control for complement activation throughout.[31,35,36,41]

For quantification of complement activation products, standard curves were constructed using the assigned concentration of each respective standard supplied by the manufacturer and validated. The slope, intercept, and correlation coefficient of the derived best-fit line for C4d, Bb, C3adesarg, C5a, and SC5b-9 standard curves were within the manufacturer's specified range. The efficacy of SWCNT treatments was established by comparison with baseline levels using paired *t*-test; correlations between two variables were analyzed by linear regression, and differences between groups (when necessary) were examined using ANOVA followed by multiple comparisons with Student−Newman−keuls test.[31,35,36,41]

Conflict of Interest: The authors declare no competing financial interest.

Acknowledgment. Financial support by the Danish Agency for Science, Technology and Innovation (Det Strategiske Forskningsråd), reference 2106-08-0081 (to S.M.M.), is gratefully acknowledged. A.J.A. is a recipient of a Ph.D. Scholarship Award from the University of Copenhagen.

REFERENCES AND NOTES

1. Iijima, S. Helical Microtubules of Graphitic Carbon. *Nature* **1991**, *354*, 56–58.
2. Ajayan, P. M. Nanotubes from Carbon. *Chem. Rev.* **1999**, *99*, 1787–1799.
3. Foldvari, M.; Bagonluri, M. Carbon Nanotubes as Functional Excipients for Nanomedicines: I. Pharmaceutical Properties. *Nanomedicine* **2008**, *4*, 173–182.

4. Bottini, M.; Rosato, N.; Bottini, N. PEG-Modified Carbon Nanotubes in Biomedicine: Current Status and Challenges Ahead. *Biomacromolecules* **2011**, *12*, 3381–3393.
5. Liu, Z.; Cai, W.; He, L.; Nakayama, N.; Chen, K.; Sun, X.; Chen, X.; Dai, H. *In Vivo* Biodistribution and Highly Efficient Tumour Targeting of Carbon Nanotubes in Mice. *Nat. Nanotechnol.* **2007**, *2*, 47–52.
6. Kam, N. W. S.; Liu, Z.; Dai, H. Carbon Nanotubes as Intracellular Transporters for Proteins and DNA: An Investigation of the Uptake Mechanism and Pathway. *Angew. Chem., Int. Ed.* **2006**, *45*, 577–581.
7. Kostarelos, K.; Lacerda, L.; Pastorin, G.; Wu, W.; Wieckowski, S.; Luangsivilay, J.; Godefroy, S.; Pantarotto, D.; Briand, J. P.; Muller, S.; *et al.* Cellular Uptake of Functionalized Carbon Nanotubes Is Independent of Functional Group and Cell Type. *Nat. Nanotechnol.* **2007**, *2*, 108–113.
8. Al-Jamal, K. T.; Gherardini, L.; Bardi, G.; Nunes, A.; Guo, C.; Bussy, C.; Herrero, M. A.; Bianco, A.; Prato, M.; Kostarelos, K.; *et al.* Functional Motor Recovery from Brain Ischemic Insult by Carbon Nanotube-Mediated siRNA Silencing. *Proc. Natl. Acad. Sci. U.S.A.* **2011**, *108*, 10952–10957.
9. Liu, Z.; Chen, K.; Davis, C.; Sherlock, S.; Cao, Q.; Chen, X.; Dai, H. Drug Delivery with Carbon Nanotubes for *In Vivo* Cancer Treatment. *Cancer Res.* **2008**, *68*, 6652–666.
10. Ji, S.-R.; Liu, C.; Zang, B.; Yang, F.; Xu, J.; Long, J.; Jin, C.; FU, D.-L.; Ni, Q.-X.; Yu, X.-J. Carbon Nanotubes in Cancer Diagnosis and Therapy. *Biochim. Biophys. Acta* **2010**, *1806*, 29–35.
11. De La Zerda, A.; Zavaleta, C.; Keren, S.; Vaithilingam, S.; Bodapati, S.; Liu, Z.; Levi, J.; Smith, B. R.; Ma, T. J.; Oralkan, O.; *et al.* Carbon Nanotubes as Photoacoustic Molecular Imaging Agents in Living Mice. *Nat. Nanotechnol.* **2008**, *3*, 557–562.
12. Liu, Z.; Tabakman, S.; Welsher, K.; Dai, H. Carbon Nanotubes in Biology and Medicine: *In Vitro* and *In Vivo* Detection, Imaging and Drug Delivery. *Nano Res.* **2009**, *2*, 85–120.
13. Robinson, J. T.; Welsher, K.; Tabakman, S. M.; Sherlock, S. P.; Wang, H.; Luong, R.; Dai, H. High Performance *In Vivo* Near-IR (>1 μm) Imaging and Photothermal Cancer Therapy with Carbon Nanotubes. *Nano Res.* **2010**, *3*, 779–793.
14. Welsher, K.; Sherlock, S. P.; Dai, H. Deep-Tissue Anatomical Imaging of Mice Using Carbon Nanotube Fluorophores in the Second Near-Infrared Window. *Proc. Natl. Acad. Sci. U.S.A.* **2011**, *108*, 8943–8948.
15. Hong, G.; Lee, J. C.; Robinson, J. T.; Raaz, U.; Xie, L.; Huang, N. F.; Cooke, J. P.; Dai, H. Multifunctional *In Vivo* Vascular Imaging Using Near-Infrared II Fluorescence. *Nat. Med.* **2012**, *18*, 1841–1846.
16. Welsher, K.; Liu, Z.; Sherlock, S. P.; Robinson, J. T.; Chen, Z.; Daranciang, D.; Dai, H. A Route to Brightly Fluorescent Carbon Nanotubes for Near-Infrared Imaging in Mice. *Nat. Nanotechnol.* **2009**, *4*, 773–780.
17. Peng, H.; Alemany, L. B.; Margrave, J. L.; Khabashesku, V. N. Sidewall Carboxylic Acid Functionalization of Single-Walled Carbon Nanotubes. *J. Am. Chem. Soc.* **2003**, *125*, 15174–15182.
18. Pompeo, F.; Resasco, D. E. Water Solubilization of Single-Walled Carbon Nanotubes by Functionalization with Glucosamine. *Nano Lett.* **2002**, *2*, 369–373.
19. Georgakilas, V.; Kordatos, K.; Prato, M.; Guldi, D. M.; Holzinger, M.; Hirsch, A. Organic Functionalization of Carbon Nanotubes. *J. Am. Chem. Soc.* **2002**, *124*, 760–761.
20. Zhao, B.; Hu, H.; Yu, A.; Perea, D.; Haddon, R. C. Synthesis and Characterization of Water Soluble Single-Walled Carbon Nanotube Graft Copolymers. *J. Am. Chem. Soc.* **2005**, *127*, 8917–8203.
21. Wang, H.; Zhou, W.; Ho, D. L.; Winey, K. I.; Fischer, J. E.; Glinka, C. J.; Hobbie, E. K. Dispersing Single-Walled Carbon Nanotubes with Surfactants: A Small Angle Neutron Scattering Study. *Nano Lett.* **2004**, *4*, 1789–1793.
22. Zheng, M.; Jagota, A.; Semke, E. D.; Diner, B. A.; McLean, R. S.; Lustig, S. R.; Richardson, R. E.; Tassi, N. G. DNA-Assisted Dispersion and Separation of Carbon Nanotubes. *Nat. Mater.* **2003**, *2*, 338–342.
23. Liu, Z.; Davis, C.; Cai, W.; He, L.; Chen, X.; Dai, H. Circulation and Long-Term Fate of Functionalized, Biocompatible Single-Walled Carbon Nanotubes in Mice Probed by Raman Spectroscopy. *Proc. Natl. Acad. Sci. U.S.A.* **2008**, *105*, 1410–1415.
24. Prencipe, G.; Tabakman, S. M.; Welsher, K.; Liu, Z.; Goodwin, A. P.; Zhang, L.; Henry, J.; Dai, H. PEG Branched Polymer for Functionalization of Nanomaterials with Ultralong Blood Circulation. *J. Am. Chem. Soc.* **2009**, *131*, 4783–4787.
25. Moghimi, S. M.; Hunter, A. C.; Andresen, T. L. Factors Controlling Nanoparticle Pharmacokinetics: An Integrated Analysis and Perspective. *Annu. Rev. Pharmacol. Toxicol.* **2012**, *52*, 481–503.
26. Moghimi, S. M.; Szebeni, J. Stealth Liposomes and Long Circulating Nanoparticles: Critical Issues in Pharmacokinetics, Opsonization and Protein-Binding Properties. *Prog. Lipid Res.* **2003**, *42*, 463–478.
27. Moghimi, S. M.; Hunter, A. C.; Murray, J. C. Nanomedicine: Current Progress and Future Prospects. *FASEB J.* **2005**, *19*, 311–330.
28. Moghimi, S. M.; Murray, J. C. Poloxamer-188 Revisited: A Potentially Valuable Immune Modulator? *J. Natl. Cancer Inst.* **1996**, *88*, 766–768.
29. Boraschi, D.; Costantino, L.; Italiani, P. Interaction of Nanoparticles with Immunocompetent Cells: Nanosafety Considerations. *Nanomedicine* **2012**, *7*, 121–131.
30. Moghimi, S. M.; Peer, D.; Langer, R. Reshaping the Future of Nanopharmaceuticals: *Ad Iudicium*. *ACS Nano* **2011**, *5*, 8454–8458.
31. Moghimi, S. M.; Hamad, I.; Andresen, T. L.; Jørgensen, K.; Szebeni, J. Methylation of the Phosphate Oxygen Moiety of Phospholipid-Methoxy(polyethylene glycol) Conjugate Prevents PEGylated Liposome-Mediated Complement Activation and Anaphylatoxin Production. *FASEB J.* **2006**, *20*, 2591–2593.
32. Moghimi, S. M.; Andersen, A. J.; Hashemi, S. H.; Lettiero, B.; Ahmadvand, D.; Hunter, A. C.; Andresen, T. L.; Hamad, I.; Szebeni, J. Complement Activation Cascade Triggered by PEG-PL Engineered Nanomedicines and Carbon Nanotubes: The Challenges Ahead. *J. Controlled Release* **2010**, *146*, 175–181.
33. Brambilla, D.; Verpillot, R.; Le Droumaguet, B.; Nicolas, J.; Taverna, M.; Kona, J.; Lettiero, B.; Hashemi, S. H.; De Kempe, L.; Canovi, M.; *et al.* PEGylated Nanoparticles Bind to and Alter Amyloid-Beta Peptide Conformation: Towards Engineering of Functional Nanomedicines for Alzheimer's Disease. *ACS Nano* **2012**, *6*, 5897–5908.
34. Rybak-Smith, M. J.; Sim, R. B. Complement Activation by Carbon Nanotubes. *Adv. Drug Delivery Rev.* **2011**, *63*, 1031–1041.
35. Hamad, I.; Hunter, A. C.; Rutt, K. J.; Liu, Z.; Dai, H.; Moghimi, S. M. Complement Activation by PEGylated Single-Walled Carbon Nanotubes is Independent of C1q and Alternative Pathway Turnover. *Mol. Immunol.* **2008**, *45*, 3797–3803.
36. Hamad, I.; Al-Hanbali, O.; Hunter, A. C.; Rutt, K. J.; Andresen, T. L.; Moghimi, S. M. Distinct Polymer Architecture Mediates Switching of Complement Activation Pathways at the Nanosphere–Serum Interface: Implications for Stealth Nanoparticle Engineering. *ACS Nano* **2010**, *4*, 6629–6638.
37. Moghimi, S. M.; Hunter, A. C. Complement Monitoring of Carbon Nanotubes. *Nat. Nanotechnol.* **2010**, *5*, 382.
38. Carrol, M. V.; Sim, R. B. Complement in Health and Disease. *Adv. Drug Delivery Rev.* **2011**, *63*, 965–975.
39. Moghimi, S. M.; Andersen, A. J.; Ahmadvand, D.; Wibroe, P. P.; Andresen, T. L.; Hunter, A. C. Material Properties in Complement Activation. *Adv. Drug Delivery Rev.* **2011**, *63*, 1000–1007.
40. Salvador-Morales, C.; Flahaut, E.; Sim, E.; Sloan, J.; Green, M. L.; Sim, R. B. Complement Activation and Protein Adsorption by Carbon Nanotubes. *Mol. Immunol.* **2006**, *43*, 193–201.
41. Hamad, I.; Hunter, A. C.; Szebeni, J.; Moghimi, S. M. Poly(ethylene glycol)s Generate Complement Activation Products in Human Serum through Increased Alternative Pathway Turnover and a MASP-2-Dependent Process. *Mol. Immunol.* **2008**, *46*, 225–232.

42. Fair, B. D.; Jamieson, A. M. Studies of Protein Adsorption on Polystyrene Latex Surfaces. *J. Colloid Interface Sci.* **1980**, *77*, 525–534.
43. Gbadamosi, J. K.; Hunter, A. C.; Moghimi, S. M. PEGylation of Microspheres Generates a Heterogeneous Population of Particles with Differential Surface Characteristics and Biological Performance. *FEBS Lett.* **2002**, *532*, 338–344.
44. Fujita, T. Evolution of Lectin-Complement Pathway and Its Role in Innate Immunity. *Nat. Rev. Immunol.* **2002**, *2*, 346–353.
45. Armstrong, J. K.; Hempel, G.; Koling, S.; Chan, L. S.; Fisher, T.; Meiselman, H. J.; Garratty, G. Antibody Against Poly-(ethylene glycol) Adversely Affects PEG-Asparginase Therapy in Acute Lymphoblastic Leukemia Patients. *Cancer* **2007**, *110*, 103–111.
46. Gaboriaud, C.; Thielens, N. M.; Gregory, L. A.; Rossi, V.; Fontecilla-Camps, J. C.; Arlaud, G. J. Structure and Activation of the C1 Complex of Complement: Unraveling the Puzzle. *Trends Immunol.* **2004**, *25*, 368–373.
47. Ling, W. L.; Biro, A.; Bally, I.; Tacnet, P.; Deniaud, A.; Doris, E.; Frachet, P.; Schoehn, G.; Pebay-Peyroula, E.; Arlaud, G. J. Proteins of the Innate Immune System Crystallize on Carbon Nanotubes but Are Not Activated. *ACS Nano* **2011**, *5*, 730–737.
48. Wallis, R. The Lectin-Pathway of Complement Activation: MBL, Other Collectins and Ficolins. *Immunobiology* **2002**, *205*, 433–445.
49. Thielens, N. M.; Gaboriaud, C.; Arlaud, G. J. Ficolins: Innate Immune Recognition Proteins for Danger Sensing. *Immunologia* **2007**, *26*, 145–156.
50. Frederiksen, P. D.; Thiel, S.; Larsen, C. B.; Jensenius, J. C. M-Ficolin, an Innate Immune Defence Molecule, Binds Patterns of Acetyl Groups and Activates Complement. *Scand. J. Immunol.* **2005**, *62*, 462–473.
51. Liu, Y.; Endo, Y.; Iwaki, D.; Nakata, M.; Matsushita, M.; Wada, I.; Inoue, K.; Munakata, M.; Fujita, T. Human M-Ficolin Is a Secretory Protein That Activates the Lectin Complement Pathway. *J. Immunol.* **2005**, *175*, 3150–3156.
52. Rybak-Smith, M. J.; Tripisciano, C.; Borowiak-Palen, E.; Lamprecht, C.; Sim, R. B. Effect of Functionalization of Carbon Nanotubes with Psychosine on Complement Activation and Protein Adsorption. *J. Biomed. Nanotechnol.* **2011**, *7*, 830–839.
53. Kemper, C.; Atkinson, J. P.; Hourcade, D. E. Properdin: Emerging Roles of a Pattern-Recognition Molecule. *Annu. Rev. Immunol.* **2010**, *28*, 131–155.
54. Wirthmueller, U.; Dewald, B.; Thelen, M.; Schafer, M. K.; Stover, A. C.; Whaley, K.; North, J.; Eggleton, P.; Reid, K. B.; Schwaeble, W. J. Properdin, a Positive Regulator of Complement Activation, Is Released from Secondary Granules of Stimulated Peripheral Blood Neutrophils. *J. Immunol.* **1997**, *158*, 4444–4451.
55. Harris, J. M. *Poly(ethylene glycol) Chemistry: Biotechnical and Biomedical Applications*; Plenum Press: New York, 1992.
56. Hattori, R.; Hamilton, K. K.; McEver, R. P.; Sims, P. J. Complement Proteins C5b-9 Induce Secretion of High Molecular-Weight Multimers of Endothelial von Willebrand-Factor and Translocation of Granule Membrane-Protein GMP-140 to the Cell-Surface. *J. Biol. Chem.* **1989**, *264*, 9053–9060.
57. Ekdahl, K. N.; Lambris, J. D.; Elwing, H.; Ricklin, D.; Nilsson, P. H.; Teramura, Y.; Nicholls, I. A.; Nilsson, B. Innate Immunity Activation on Biomaterial Surfaces: A Mechanistic Model and Coping Strategies. *Adv. Drug Delivery Rev.* **2011**, *63*, 1042–1050.
58. Dobrovolskaia, M. A.; McNeil, S. E. Immunological Properties of Engineered Nanomaterials. *Nat. Nanotechnol.* **2007**, *2*, 469–478.
59. Sun, X.; Zaric, S.; Daranciang, D.; Welsher, K.; Lu, Y.; Li, X.; Dai, H. Optical Properties of Ultrashort Semiconducting Single-Walled Carbon Nanotube Capsules Down to Sub-10 nm. *J. Am. Chem. Soc.* **2008**, *130*, 6551–6555.
60. Tan, S. M.; Chung, M. C. M.; Kon, O. L.; Thiel, S.; Lee, S. H.; Lu, J. Improvements on the Purification of Mannan-Binding Lectin and Demonstration of Its Ca^{2+}-Independent Association with a C1s-like Serine Protease. *Biochem. J.* **1996**, *319*, 329–332.